Applied Clay Science 127–128 (2016) 129–133

Contents lists available at ScienceDirect

Applied Clay Science

journal homepage: www.elsevier.com/locate/clay

Research paper

Study of spatial distribution of sepiolite in sepiolite/polyamide6,6 nanocomposites

Cristina Fernandez-Barranco [a,*], Anna E. Kozioł [b], Krzysztof Skrzypiec [b], Michał Rawski [b], Marek Drewniak [b], Africa Yebra-Rodriguez [a]

[a] Department of Geology and CEACTierra, University of Jaen, Campus Las Lagunillas s/n, 23071 Jaen, Spain
[b] Departament of Crystallography, Maria Curie-Sklodowska University, Maria Curie Sklodowska Square 3, Lublin 20-031, Poland

ARTICLE INFO

Article history:
Received 31 August 2015
Received in revised form 14 April 2016
Accepted 18 April 2016
Available online 25 April 2016

Keywords:
Sepiolite
Nanocomposites
Polyamide6,6
Dispersion

ABSTRACT

The enhancement of the technical properties of a Clay/Polymer Nanocomposite (CPN) is related to the homogeneity and dispersion of the filler within the polymer matrix. In this work, samples of pure polyamide 6,6 (PA66) and reinforced PA66 with 1, 3, 5, 7 and 9 wt.% of sepiolite have been studied. The samples have been qualitatively analyzed with different microscopy techniques and with X-Ray diffraction and scattering techniques. The images obtained by confocal microscopy show that the sepiolite is homogeneously distributed in the PA66 matrix. The micrographs taken by scanning electron microscopy (SEM) and transmission electron microscopy (TEM) show that sepiolite fibres are oriented and equidistantly distributed even in the samples with high percentages of sepiolite. TEM images reveal the absence of clusters of sepiolite and good dispersion of the reinforcement within the matrix. The quantification of the dispersion, calculated from the results of Small Angle X-Ray Scattering (SAXS), indicates that the polymer chains are expanded due to the arrangement of sepiolite within the PA66 matrix and that the fibres are properly dispersed in the polymer.

1. Introduction

The number of industrial applications that requires new and improved materials has been increasing in the last decade. Since Toyota's first patent in the 80s of the last century (Okada et al., 1987), specific efforts have been devoted to Clay/Polymer Nanocomposites (CPN). CPN show enhanced technical properties respect to the counterparts, e.g. mechanical (Kojima et al., 1993), optical (Soulestin et al., 2012), thermal stability (Zabaleta et al., 2011) and barrier properties (Yeh et al., 2009), among others. Thus, CPN are used in aerospace (Balakrishnan and Raghavan, 2003), automotive (Hong et al., 2005) and textile (Joshi et al., 2005) industries. The enhancement of these properties is highly dependent of the extent of exfoliation of the filler into their primary nanometer scale size (LeBaron et al., 1999; Alix et al., 2012). For that reason, layered phylosillicates like montmorillonite have been widely used for the production of polymer/clay nanocomposites based on different polymer matrices (Mittal, 2009 and references therein). There are several methods to synthetize CPN as intercalated or exfoliated structure, using a variety of surfactants, dispersion techniques and polymerization conditions (Usuki et al., 2005; Nguyen and Baird, 2006). Melt intercalation is a simple method to achieve high dispersion degree in the resulting hybrids (Liu et al., 1999; Dennis et al., 2001; Fornes et al., 2002). In addition, this method provides the reproducibility needed in the manufacture of materials at the industrial scale (such as extrusion or injection molding).

Recently, the fibrous clay mineral sepiolite has been taken into consideration for the manufacture of thermoplastic matrix nanocomposites (Garcia-Lopez et al., 2010; Yu et al., 2011; Chen et al., 2012; Fukushima et al., 2012; Fernandez-Barranco et al., 2015). Sepiolite ($Mg_8(OH)_4Si_{12}O_{30}\cdot nH_2O$) organizes in T-O-T layers consisting in two sheets of SiO_4 tetrahedrons in which the unshared oxygen atoms face each other. The tetrahedral sheets are bonded with a discontinuous octahedral sheet in which magnesium atoms are coordinated. Hence the structure contains open channels (zeolitic channels) with zeolitic water (Jones and Galan, 1988). The size of the sepiolite fibres ranges between 0.5 and 7 μm and the specific surface area is estimated around 900 m^2/g (Martinez-Martinez et al., 2011).

Although some montmorillonite based nanocomposites are already commercially used (e.g. with polyamide6 matrix in Mitsubishi GDI motors, polyolefine matrix in the Chevrolet Astro, among others), some fundamental studies have to be performed in sepiolite/polymer nanocomposites prior to the commercial use of these materials in order to better control their properties and behavior. The aim of this work is to evaluate the spatial distribution in sepiolite/polyamide6,6 (sep/PA66) nanocomposites with different reinforcement loading manufactured via melt intercalation. For that purpose, different microscopy techniques were used in order to obtain images with different magnifications and reveal the different phases. Moreover, the extent of dispersion of the sepiolite filler was analyzed with X-Ray diffraction

* Corresponding author.
E-mail address: cfernand@ujaen.es (C. Fernandez-Barranco).

http://dx.doi.org/10.1016/j.clay.2016.04.015
0169-1317/

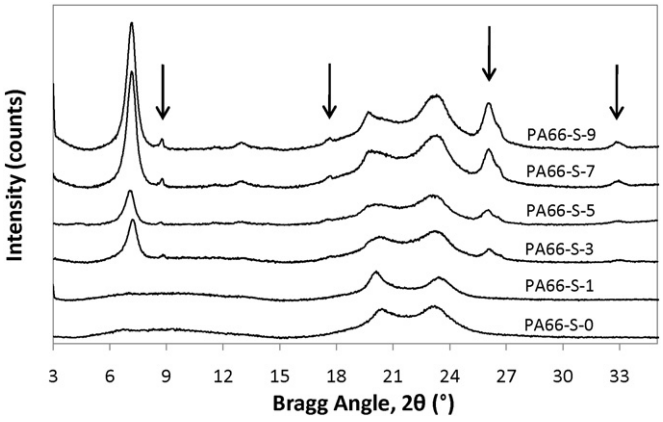

Fig. 1. XRD patterns of CPN samples with different sepiolite loading (the curves have been vertically displaced for clarity). The arrows represent the characteristic diffraction peaks of the hybrid structure sep/PA66.

and scattering techniques and quantified using the electron density difference.

2. Materials and methods

CPN samples were manufactured via melt intercalation of commercial polyamide6,6 (PA66, Dinalon®, Grupo Repol, Spain) and sepiolite organophilized with dimethyl di(hydroxytallow) ammonium chloride (Tolsa S.A., Spain). Different weight percent of organophilized sepiolite as reinforcing agent were used. The pellets were obtained using a double screw extruder (250 rpm, 250 °C). After this process, the pellets were injection molded into plates 2 mm thickness in a BABYPLAST 6/10, CRONOPLAST at 25 MPa, 285 °C in the cylinder and 50 °C tool temperature. The obtained nanocomposites were PA66-S-1, PA66-S-3, PA66-S-5, PA66-S-7 and PA66-S-9, with 1, 3, 5, 7 and 9 sepiolite wt.%, respectively. The neat PA66 (sample PA66-S-0) was also extruded prior to the injection molding process to guarantee identical manufacture conditions (stress and temperature treatment during processing).

X-Ray diffraction (XRD) patterns of the samples were collected in a X-Ray Empyrean Diffractometer with PIXcel-3D detector (PANalytical, The Netherlands), with the following experimental conditions: CuKα radiation (1.54178 Å), 40 kV, 35 mA and 2θ range between 3 and 35°. Microphotographs were taken with the help of different microscopy techniques. A confocal microscope (Nikon D-ECLIPSE C1) was used, equipped with objectives Nikon LU PLAN FLUOR and laser with 488 nm wavelength and 50 mW power as light source. The resolution of the scans was 1024 × 1024 pixels. The data were analyzed with the EZ-C1 Gold Software (version 3.90 build 869). Scanning Electron Microscopy (SEM) images were obtained in a microscope Quanta 3D FEG, detection LVSED at 30 kV and 80 Pa pressure. Images were also obtained in a Transmission Electron Microscope (TEM JEOL JEM-1010) with a camera Gatan mod. 782 and DigitalMicrograph software at 80 kV voltage. Prior to the TEM analyses, the samples were cut with an ultramicrotome Leica UC7 equipped with a diamond blade of 45°. The thickness of the cuttings ranged between 70 and 100 nm. Small Angle X-Ray Scattering (SAXS) was performed in a compact Kratky camera equipped with the SWAXS optical system of HECUSMBRAUN (Austria) at the following experimental conditions: Cu radiation, Ni filter, UZ40 kV and IZ30 mA (PW1830 Philips generator). The scattered radiation was detected by the linear position sensitive counter OED-51. The resolution of the measurements was 750 Å.

3. Results and discussion

The XRD patterns of neat polyamide6,6 and CPN samples are shown in Fig. 1. The most representative diffraction peaks of PA66 appear at 20.50 and 23.28°2θ, which indicate the presence of the PA66 α-phase. The peak at 20.50°2θ (d = 4.328 Å) corresponds to the diffraction of the (100) plane. The second peak (d = 3.818 Å) results from the diffraction on two planes (010/110). The broad shoulder at 4–14°2θ appears in the sample PA66-S-0 and PA66-S-1 due to the diffraction on the disordered lattice planes (001) and (002) of the α-phase (Bunn and Garner, 1947). The diffraction peaks at 8.70, 17.55, 26.03 and 32.86°2θ correspond to the microstructure of the hybrid. These peaks are more intense at increasing percentage of sepiolite content. In addition, an intense peak at 7.04°2θ (attributed to the (110) plane of sepiolite, Brauner

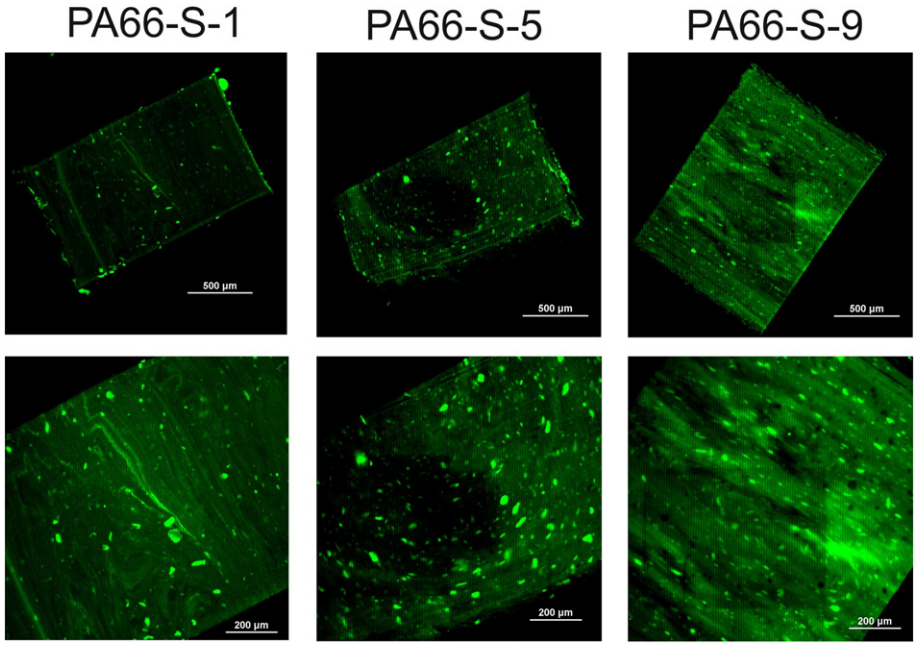

Fig. 2. Confocal images of some selected samples, where the fluorescent character (green parts) of the reinforcement can be observed. From left to right: PA66-S-1, PA66-S-5 and PA66-S-9.